

Publications

12-1-2005

**Measuring the Evolution of the Most Stable Optical Clock G
117-B15A**

S. O. Kepler

Instituto de Física, Universidade Federal do Rio Grande do Sul

Ted von Hippel

University of Texas at Austin, vonhippt@erau.edu

et al.

Follow this and additional works at: <https://commons.erau.edu/publication>



Part of the [Stars, Interstellar Medium and the Galaxy Commons](#)

Scholarly Commons Citation

Kepler, S. O., von Hippel, T., & al., e. (2005). Measuring the Evolution of the Most Stable Optical Clock G 117-B15A. *The Astrophysical Journal*, 634(2). Retrieved from <https://commons.erau.edu/publication/252>

This Article is brought to you for free and open access by Scholarly Commons. It has been accepted for inclusion in Publications by an authorized administrator of Scholarly Commons. For more information, please contact commons@erau.edu.

MEASURING THE EVOLUTION OF THE MOST STABLE OPTICAL CLOCK G 117-B15A

S. O. KEPLER, J. E. S. COSTA, AND B. G. CASTANHEIRA

Instituto de Física da UFRGS, 91501-900 Porto Alegre RS, Brazil; kepler@if.ufrgs.br

D. E. WINGET, FERGAL MULLALLY, R. E. NATHER, MUKREMIN KILIC, AND TED VON HIPPEL

Department of Astronomy and McDonald Observatory, University of Texas, Austin, TX 78712

ANJUM S. MUKADAM

Department of Astronomy, University of Washington, Seattle, WA 98195-1580

AND

DENIS J. SULLIVAN

School of Chemical and Physical Sciences, Victoria University of Wellington, New Zealand

Received 2005 June 1; accepted 2005 July 28

ABSTRACT

We report our measurement of the rate of change of period with time (\dot{P}) for the 215 s periodicity in the pulsating white dwarf G 117-B15A, the most stable optical clock known. After 31 years of observations, we have finally obtained a 4σ measurement $\dot{P}_{\text{observed}} = (4.27 \pm 0.80) \times 10^{-15} \text{ s s}^{-1}$. Taking into account the proper-motion effect of $\dot{P}_{\text{proper}} = (7.0 \pm 2.0) \times 10^{-16} \text{ s s}^{-1}$, we obtain a rate of change of period with time of $\dot{P} = (3.57 \pm 0.82) \times 10^{-15} \text{ s s}^{-1}$. This value is consistent with the cooling rate in our white dwarf models only for cores of C or C/O. With the refinement of the models, the observed rate of period change can be used to accurately measure the ratio of C/O in the core of the white dwarf.

Subject headings: stars: evolution — stars: individual (G117-B15A) — stars: oscillations

Online material: machine-readable table

1. INTRODUCTION

G 117-B15A is a pulsating white dwarf with a hydrogen atmosphere, a DAV, also called a ZZ Ceti star (McGraw 1979). These stars show multiperiodic nonradial g -mode pulsations that can be used to measure their internal properties and rate of evolution.

McGraw & Robinson (1976) found that the star was variable, and Kepler et al. (1982) studied its light curve, finding six simultaneous pulsations. The dominant mode has a period of 215 s and a fractional amplitude of 22 mma (milli-modulation amplitude = $1/1.086$ millimagnitude), and it is stable in amplitude and phase. The other smaller pulsation modes vary in amplitude from night to night (Kepler et al. 1995), suggesting the presence of unresolved components. Because the DAVs appear to be normal stars except for their variability (Robinson 1979; Bergeron et al. 1995, 2004), i.e., an evolutionary stage in the cooling of all white dwarfs, it is likely that the DAV structural properties are representative of *all* DA white dwarfs.

Mukadam et al. (2004b) and Mullally et al. (2005) discovered 46 new ZZ Ceti stars and more than doubled the number of known variables, using T_{eff} and $\log g$ values derived from the optical spectra obtained by the Sloan Digital Sky Survey (Kleinman et al. 2004). While Bergeron et al. (1995, 2004) find the ZZ Ceti instability strip to be pure, i.e., contain no nonvariable stars, Mukadam et al. (2004a, 2004b) and Mullally et al. (2005) find several stars inside the instability strip for which they could detect no variability above their detection threshold. It is necessary to obtain $S/N \geq 50$ spectra of the nonvariables within the strip and reanalyze their T_{eff} and $\log g$ values, and also to obtain additional time series photometry on these stars, to ensure that they are not low amplitude variables, and restudy the purity of the instability strip.

We report our continuing study of the star G 117-B15A, also called RY LMi and WD 0921+354, one of the hottest of the ZZ Ceti stars. We expect that the rate of change of a pulsation period

with time for g -mode pulsations in white dwarf stars to be directly related to its evolutionary timescale (Winget et al. 1983), allowing us to infer the age of a cool white dwarf since its formation. We have been observing the star since 1974 to measure the rate of period change with time (\dot{P}) for the largest amplitude periodicity. Using all the data obtained from 1974 through 1999, Kepler et al. (2000) arrived at a determination of $\dot{P} = (2.3 \pm 1.4) \times 10^{-15} \text{ s s}^{-1}$.

G 117-B15A was the first pulsating white dwarf to have its main pulsation mode index identified. The 215 s mode is an $\ell = 1$, as determined by comparing the ultraviolet pulsation amplitude (measured with the *Hubble Space Telescope* [HST]) to the optical amplitude (Robinson et al. 1995). Kotak et al. (2004) confirm the ℓ measurement for the $P = 215$ s pulsation and show that the other large-amplitude modes, at 271 and 304 s, show chromatic amplitude changes that do not fit the theoretical models, using time-resolved spectra obtained at the Keck Telescope. Robinson et al. (1995), and Koester et al. (1994) derive T_{eff} near 12,400 K, while Bergeron et al. (1995, 2004), using a less efficient model for convection, derive $T_{\text{eff}} = 11,630$ K.

Kepler (1984) demonstrated that the observed variations in the light curve of G 117-B15A are due to nonradial g -mode pulsations. Kepler et al. (2000) show that the models predict the effect of radius change due to still ongoing contraction to be an order of magnitude smaller than the cooling effect on the rate of period change.

G 117-B15A is proving to be a useful laboratory for particle physics (Isern et al. 2004). Córscico et al. (2001) calculate the limit on the axion mass compatible with the then-observed upper limit to the cooling, showing $m_a \cos \beta \leq 4.4$ meV, and Kepler (2004) demonstrates that axion cooling would be dominant over neutrino cooling for the lukewarm white dwarf stars for axion masses of this order. Biesiada & Malec (2002) show that the 2σ upper limit published in Kepler et al. (2000) limits the string mass scale

$M_S \geq 14.3 \text{ TeV}/c^2$ for six dimensions, from the observed cooling rate and the emission of Kaluza-Klein gravitons, but the limit is negligible for higher dimensions. Benvenuto et al. (2004) show the observed rates of period change can also be used to constrain the dynamical rate of change of the constant of gravity \dot{G} .

Bradley (1996, 1998) use the mode identification and the observed periods of the three largest known pulsation modes to derive a hydrogen layer mass lower limit of $10^{-6} M_*$ and a best estimate of $1.5 \times 10^{-4} M_*$, assuming $k = 2$ for the 215 s mode and a 20:80 C/O core mass. The core composition is constrained mainly by the presence of the 304 s pulsation. Benvenuto et al. (2002) show that the seismological models with time-dependent element diffusion are only consistent with the spectroscopic data if the modes are the $\ell = 1, k = 2, 3$, and 4, and deduce that $M = 0.525 M_\odot$, $\log(M_H/M_*) \geq -3.83$, and $T_{\text{eff}} = 11,800 \text{ K}$. Their best model predicts, for parallax $\Pi = 15.89 \text{ mas}$, $\dot{P} = 4.43 \times 10^{-15} \text{ s s}^{-1}$ for $P = 215 \text{ s}$, $\dot{P} = 3.22 \times 10^{-15} \text{ s s}^{-1}$ for $P = 271 \text{ s}$, and $\dot{P} = 5.76 \times 10^{-15} \text{ s s}^{-1}$ for the $P = 304 \text{ s}$ periodicities.

2. OBSERVATIONS

Kepler et al. (2000) reported on the observations from 1974 to 2000. We report in this paper an additional 19.3 hr of time series photometry in 2001, 30.6 hr in 2002, 24.4 hr in 2003, 4 hr in 2004, and 13.6 hr in 2005, most using the Argos prime-focus CCD camera (Nather & Mukadam 2004) on the 2.1 m Otto Struve telescope at McDonald Observatory.

We observed the light through a BG40 filter to maximize the signal-to-noise ratio (S/N) because the pulsation amplitudes are small (2%), the star is faint ($V = 15.52$; Eggen & Greenstein 1965), and also because the nonradial g -mode light variations have the same phase in all colors (Robinson et al. 1982) but the amplitudes decrease with wavelength. For example, a filterless observation with Argos gives an amplitude around 40% smaller for G 117-B15A.

3. DATA REDUCTION

We reduce and analyze the data in the manner described by Nather et al. (1990) and Kepler (1993). We bring all the data to the same fractional amplitude scale, and the times from UTC to the uniform Barycentric Julian Coordinated Date (TCB) scale, using JPL DE405 ephemeris (Standish 1998, 2004) to model Earth's motion. We compute Fourier transforms for each individual run and verify that the main pulsation at 215 s dominates each data set and has an amplitude stable up to 15%, our uncertainty in amplitude due to the lack of accurate time- and color-dependent extinction determination.

4. TIMESCALE FOR PERIOD CHANGE

As the dominant pulsation mode at $P = 215 \text{ s}$ has had a stable frequency and amplitude since our first observations in 1974, we can calculate the time of maximum for each new run and look for deviations.

We fit our observed time of maximum light (O) to the calculated (C) by the equation

$$(O - C) = \Delta E_0 + \Delta PE + \frac{1}{2} P \dot{P} E^2,$$

where $\Delta E_0 = (T_{\text{max}}^0 - T_{\text{max}}^1)$, $\Delta P = (P - P_{t=T_{\text{max}}^0})$, E is the epoch of the time of maximum, i.e., the integer number of cycles after our first observation, T_{max}^0 is the time of maximum assumed, T_{max}^1 is the time of maximum that best fit the parabola, P is the period that best fit the parabola, and $P_{t=T_{\text{max}}^0}$ is the period assumed

TABLE 1
TOTAL DATA SET TO DATE

Time of Maximum (BJDD)	Epoch of Maximum	($O - C$) (s)	σ (s)
2442397.917507.....	0	0.0	2.1
2442477.797089.....	32071	0.5	1.7
2442779.887934.....	153358	3.9	2.1
2442783.850624.....	154949	1.2	2.9
2442786.981458.....	156206	2.2	1.5
2443462.962774.....	427607	1.6	1.4
2443463.946592.....	428002	0.5	1.4
2443465.969049.....	428814	0.5	1.6
2443489.909755.....	438426	0.2	1.5
2443492.898616.....	439626	0.9	1.6
2443521.927837.....	451281	0.1	1.3
2443552.752879.....	463657	0.8	1.4
2443576.725940.....	473282	-1.6	3.3
2443581.692438.....	475276	0.3	1.3
2443582.693698.....	475678	-0.2	1.3
2443583.697469.....	476081	1.0	1.3
2443584.733602.....	476497	0.8	1.4
2443604.659292.....	484497	1.3	1.5
2443605.752703.....	484936	0.4	1.4
2443611.693050.....	487321	0.6	1.3
2443613.658222.....	488110	0.7	1.6
2443636.674971.....	497351	8.8	3.4
2443839.956765.....	578967	5.8	3.0
2443841.976708.....	579778	3.7	3.5
2443842.980413.....	580181	-0.7	2.2
2443843.944332.....	580568	0.5	2.6
2443869.989703.....	591025	1.5	2.4
2443870.946182.....	591409	5.5	3.1
2443874.916339.....	593003	2.4	2.1
2443959.695117.....	627041	0.1	2.0
2443963.662836.....	628634	1.6	2.1
2443990.664641.....	639475	2.7	1.3
2444169.945954.....	711455	0.1	1.6
2444231.822666.....	736298	-0.7	2.9
2444232.818992.....	736698	3.0	1.6
2444293.833896.....	761195	0.3	1.8
2444637.776174.....	899285	5.8	1.9
2444641.624287.....	900830	2.8	1.1
2444992.789531.....	1041820	0.1	1.6
2444994.689956.....	1042583	1.2	1.2
2444996.744801.....	1043408	2.0	1.3
2444997.723649.....	1043801	1.9	1.2
2445021.716661.....	1053434	1.7	1.4
2445703.860004.....	1327309	1.9	1.7
2445734.642701.....	1339668	2.4	1.2
2445735.643972.....	1340070	2.8	1.3
2446113.763716.....	1491882	2.9	1.2
2446443.775386.....	1624379	2.8	1.1
2446468.630178.....	1634358	2.1	1.3
2446473.718679.....	1636401	0.3	1.6
2446523.620086.....	1656436	2.2	1.6
2446524.613917.....	1656835	5.5	2.5
2446768.855451.....	1754896	2.9	1.4
2446794.935676.....	1765367	2.5	2.1
2446796.928219.....	1766167	0.3	1.6
2446797.924535.....	1766567	3.1	1.3
2446798.903378.....	1766960	2.6	1.8
2446823.663537.....	1776901	3.1	1.9
2446825.651132.....	1777699	3.7	1.5
2447231.328096.....	1940575	3.7	1.9
2447231.612054.....	1940689	5.1	3.5
2447232.396626.....	1941004	5.0	1.6
2447232.623291.....	1941095	5.9	2.9
2447233.343090.....	1941384	4.5	1.3

TABLE 1—Continued

Time of Maximum (BJDD)	Epoch of Maximum	($O - C$) (s)	σ (s)
2447233.634506.....	1941501	4.7	2.3
2447234.319475.....	1941776	6.8	3.2
2447235.313250.....	1942175	5.2	1.4
2447235.607168.....	1942293	6.4	2.1
2447236.610922.....	1942696	6.2	1.6
2447589.375198.....	2084328	3.2	1.4
2447594.331735.....	2086318	5.2	1.6
2447595.323018.....	2086716	3.5	2.0
2447596.311907.....	2087113	10.1	2.3
2447597.315602.....	2087516	4.8	1.7
2447598.319339.....	2087919	3.1	3.1
2447499.072036.....	2048072	6.5	3.2
2447532.768799.....	2061601	1.3	1.4
2447853.846325.....	2190511	4.3	2.1
2447856.832697.....	2191710	5.2	1.9
2447918.644630.....	2216527	2.6	3.1
2447920.619811.....	2217320	6.7	3.3
2447952.622834.....	2230169	-3.3	2.9
2447972.620899.....	2238198	9.6	6.1
2447973.709340.....	2238635	9.7	2.6
2447973.741682.....	2238648	6.5	1.4
2447978.770467.....	2240667	10.0	2.1
2447979.781717.....	2241073	11.8	3.1
2447980.319627.....	2241289	4.6	3.5
2447977.403038.....	2240118	7.5	2.3
2447978.327055.....	2240489	4.3	3.3
2447979.358189.....	2240903	2.6	3.4
2447979.358145.....	2240903	-1.2	4.9
2447978.601069.....	2240599	7.4	2.5
2447980.621017.....	2241410	5.8	3.4
2447980.782929.....	2241475	7.2	2.3
2447981.325918.....	2241693	8.4	1.4
2447981.592393.....	2241800	5.7	1.4
2447981.779185.....	2241875	4.8	1.1
2447982.329663.....	2242096	7.4	1.8
2447982.743093.....	2242262	5.0	1.2
2447983.734400.....	2242660	5.4	1.2
2447979.281057.....	2240872	9.5	2.9
2447980.224899.....	2241251	-2.4	2.9
2447984.735678.....	2243062	6.5	1.1
2448245.724666.....	2347847	-3.3	5.1
2448267.799932.....	2356710	5.2	2.3
2448324.627972.....	2379526	4.3	1.2
2448325.708938.....	2379960	4.1	1.3
2448328.593208.....	2381118	6.4	1.6
2448331.661735.....	2382350	4.0	1.2
2448238.571479.....	2344975	8.3	2.2
2448622.833258.....	2499253	3.3	1.8
2448680.642683.....	2522463	6.3	1.2
2448687.614155.....	2525262	4.0	1.2
2448688.597979.....	2525657	3.4	1.2
2449062.660365.....	2675840	4.2	1.6
2449063.609354.....	2676221	6.7	1.9
2449066.615640.....	2677428	6.5	1.4
2449066.371558.....	2677330	7.2	2.0
2449066.326737.....	2677312	8.2	2.6
2449069.342967.....	2678523	6.4	1.7
2449298.239287.....	2770423	8.5	4.1
2449298.304041.....	2770449	8.2	4.1
2449294.214264.....	2768807	5.5	4.1
2449294.293897.....	2768839	-0.5	4.1
2449295.439583.....	2769299	-4.0	6.1
2449295.494387.....	2769321	-3.3	7.1
2449036.809260.....	2665461	2.4	2.2

TABLE 1—Continued

Time of Maximum (BJDD)	Epoch of Maximum	($O - C$) (s)	σ (s)
2449038.677300.....	2666211	3.1	2.2
2449040.687310.....	2667018	3.6	4.1
2449041.616360.....	2667391	4.9	4.1
2449799.723888.....	2971765	5.6	1.3
2450427.920960.....	3223981	8.2	3.8
2450429.973242.....	3224805	2.7	2.4
2450430.914779.....	3225183	6.9	2.5
2450431.843821.....	3225556	7.5	1.5
2450434.912392.....	3226788	8.8	2.0
2450436.929828.....	3227598	5.4	1.7
2450483.633189.....	3246349	9.6	1.8
2451249.5989069.....	3553878	10.1	1.3
2451249.7632895.....	3553944	9.7	1.7
2451250.6126098.....	3554285	8.7	2.0
2451526.8772586.....	3665203	10.4	1.2
2451528.8523866.....	3665996	10.0	1.5
2451528.9196061.....	3666023	7.4	1.4
2451528.9868422.....	3666050	6.3	1.9
2451529.8585943.....	3666400	6.6	2.0
2451530.9097492.....	3666822	13.4	2.41
2451960.8561629.....	3839442	10.1	1.62
2451962.7864775.....	3840217	11.3	1.48
2451967.6806926.....	3842182	8.1	1.93
2451988.7919772.....	3850658	10.5	2.00
2451990.7845255.....	3851458	8.8	1.59
2452037.6472583.....	3870273	10.1	3.39
2452045.6399770.....	3873482	12.5	1.85
2452225.9050927.....	3945857	7.6	1.34
2452225.9598927.....	3945879	8.0	0.65
2452263.8834810.....	3961105	10.6	0.58
2452316.6442205.....	3980721	13.1	1.0
2452317.8995164.....	3982288	12.2	0.67
2452319.7999417.....	3982691	12.0	0.79
2452317.6479750.....	3982792	10.3	0.95
2452321.8348344.....	3983555	11.4	1.23
2452322.7265266.....	3984372	9.9	3.03
2452312.7412881.....	3980721	13.1	1.0
2452316.6442205.....	3982288	12.2	0.67
2452317.6479750.....	3982691	12.0	0.79
2452317.8995164.....	3982792	10.3	0.95
2452319.7999417.....	3983555	11.4	1.23
2452321.8348344.....	3984372	9.9	3.03
2452322.7265266.....	3984730	11.4	3.5
2452584.8812628.....	4089983	9.9	1.1
2452585.9821875.....	4090425	12.6	1.2
2452586.8937641.....	4090791	10.6	0.68
2452665.7845581.....	4122465	12.8	1.0
2452669.7970851.....	4124076	12.5	1.23
2452696.8561592.....	4134940	12.0	1.83
2452702.7043413.....	4137288	11.5	1.74
2452720.6748446.....	4144503	13.8	0.92
2452724.6624548.....	4146104	12.3	0.7
2452731.7584853.....	4148953	12.0	1.16
2452997.8983947.....	4255806	13.7	0.72
2452999.0291414.....	4256260	10.6	1.52
2453002.7851586.....	4257768	12.8	0.96
2453026.7607115.....	4267394	10.5	0.81
2453381.7442572.....	4409917	11.5	1.41
2453439.7653860.....	4433212	13.9	1.0
2453446.6073830.....	4435959	14.9	0.71
2453473.6191370.....	4446804	15.1	0.75

NOTE.—Table 3 is also available in machine-readable form in the electronic edition of the *Astrophysical Journal*.

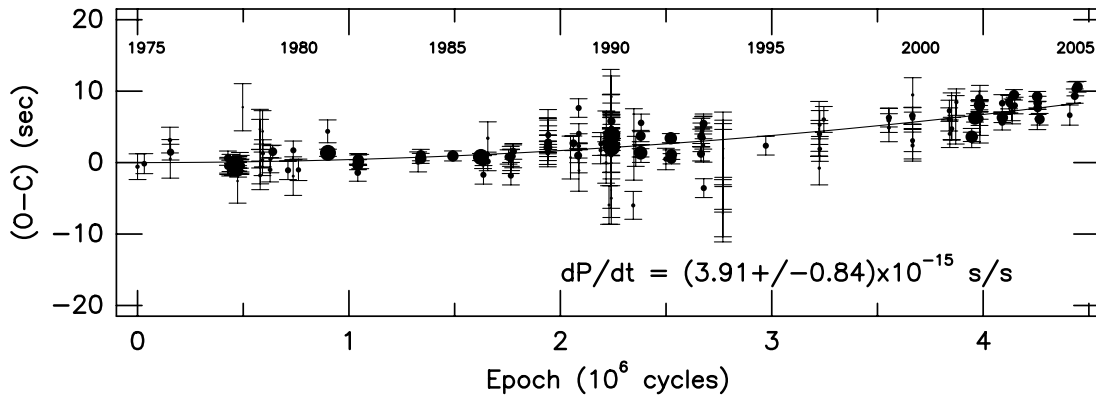


FIG. 1.— $(O - C)$ (observed minus calculated times of maxima) for the 215 s pulsation of G 117-B15A. The size of each point is proportional to its weight, i.e., inversely proportional to the uncertainty in the time of maxima squared. We show 2σ error bars for each point, and the line shows our best-fit parabola to the data. The error bars plotted are those before adding the external uncertainty of 1 s quadratically, discussed in the text. The fact the line does not overlap these error bars demonstrates that they are underestimates. Note that as the period of pulsation is 215.197 s, the whole plot shows only $\pm 36^\circ$ in phase.

at T_{\max}^0 .¹ The times of maxima are calculated by a linear least-squares fit of the light curve of each night to a sum of the six detected frequencies. They are shown in Table 1.

In Figure 1, we show the $O - C$ timings after subtracting the correction to period and epoch, and our best-fit curve through

¹ Fitting the whole light curve with a term proportional to $\sin\{[2\pi/(P + \frac{1}{2}\dot{P})]t + \phi\}$ by nonlinear least squares gives unreliable uncertainty estimates, and the alias space in P and \dot{P} is extremely dense due to the 31 yr data set span (O'Donoghue 1994; Costa et al. 1999). Our nonlinear least-squares result is $\dot{P} = (3.38 \pm 0.0013) \times 10^{-15} \text{ s s}^{-1}$.

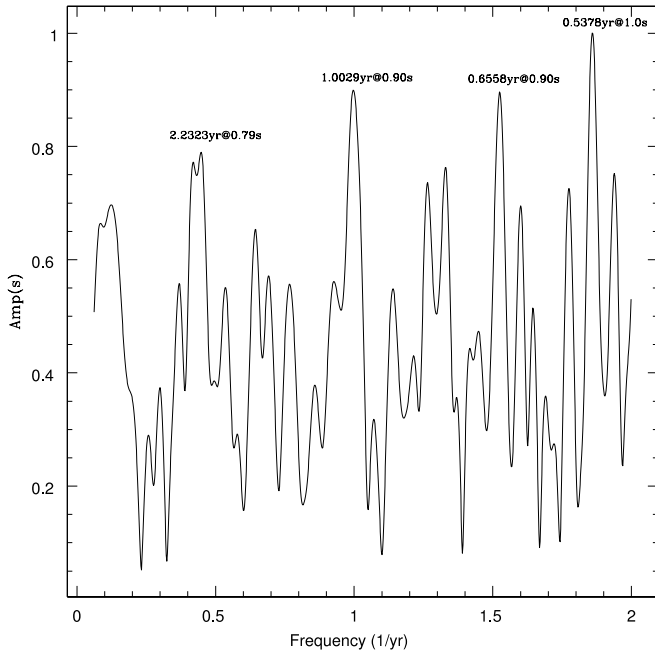


FIG. 2.—Fourier transform of $O - C$ (observed minus calculated times of maxima) for the 215 s pulsation of G 117-B15A, after we subtract the parabola. Kepler's law (1616) shows that $a_* \simeq (M_p/M_*)^{2/3} (G/4\pi^2)^{1/3} P^{2/3}$, considering $M_p \ll M_*$, from which we get $a_* \simeq 0.565 (M_p/M_*) P^{2/3}$ (with a_* in units of light-seconds and P in units of years), i.e., a 1 s light travel time, as the limit shows, for planets with masses between $1.6M_J$ and $0.27M_J = 87 M_\oplus$, for periods between 6 months and 7 yr, respectively. The highest peak, at a frequency of 1.85 yr^{-1} , corresponding to a period of 6.5 months, is extremely hard to study in our data set, as we normally observe for only 3 months separated by 1 yr. These variations can be caused by the beating of very closely spaced pulsations (Kepler et al. 1995), and we must take into account that multiplets cause nonsinusoidal variations, as the triplet in G 226-29 studied by Kepler et al. (1983).

the data. The size of each point is proportional to its weight, i.e., inversely proportional to the square of uncertainty in phase. The error bars plotted are $\pm 1\sigma$. From our data through 2005, we obtain a new value for the epoch of maximum, $T_{\max}^0 = 2442397.9175141 \text{ TCB} \pm 0.41 \text{ s}$, a new value for the period, $P = 215.1973888 \pm 0.0000004 \text{ s}$, and most importantly, a rate of period change of

$$\dot{P} = (4.27 \pm 0.80) \times 10^{-15} \text{ s s}^{-1}.$$

We use linear least squares to make our fit, with each point weighted inversely proportional to the uncertainty in the time of maxima for each individual run squared. We quadratically add an additional 1 s of uncertainty to the time of maxima for each night to account for external uncertainty caused perhaps by the beating of possible small-amplitude pulsations (Kepler et al. 1995) or the small modulation seen in Figure 1. The amplitude, 1 s, is chosen from the Fourier transform of the $O - C$ times shown in Figure 2 and is in agreement with the Kopeikin & Potapov (2004) conclusion that the Fourier analysis of the times of arrival (TOAs) gives unbiased information about the noise. Such external uncertainty is also consistent with Splaver et al. (2005), who show that the true uncertainties of the TOAs of the milli-second pulsars are generally larger than the formal uncertainties and that a quadratic term is added to them to fit the observations.

5. DISCUSSION

While it is true that the period change timescale can be proportional to the cooling timescale, it is also possible that other phenomena with shorter timescales can affect \dot{P} . The cooling timescale is the longest possible one.

As a corollary, if the observed \dot{P} is low enough to be consistent with evolution, then other processes, such as perhaps a magnetic field or diffusion induced changes in the boundary layers, are not present at a level sufficient to affect \dot{P} .

For the first time we also report on the search for the rates of period changes for the other relatively large amplitude modes of G 117-B15A, $dP/dt = (36.0 \pm 7.2) \times 10^{-15} \text{ s s}^{-1}$ for the 270 s periodicity, and $dP/dt = (74 \pm 15) \times 10^{-15} \text{ s s}^{-1}$ for the 304 s periodicity. They are much larger than the one derived for the main pulsation, which has a region of period formation deeper in the core, but are in line with the measurements for the 274 s modes in ZZ Ceti (Mukadam et al. 2003). The models to date, without rotation, differential rotation, and magnetic fields, do not explain such values, or the chromatic amplitude changes reported by Kotak

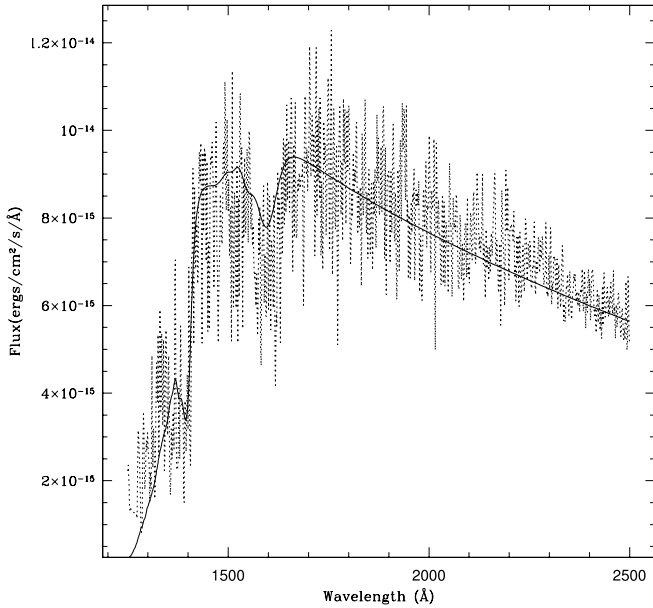


FIG. 3.—Fit of a model atmosphere with $T_{\text{eff}} = 12,000$ K, $\log g = 8.0$, $d = 67$ pc, to the *HST* FOS spectrum of G 117-B15A.

et al. (2004). Kepler et al. (1995) show that the 270 and 304 s periodicities have significant amplitude changes, indicative of multiple components or resonances.

5.1. Theoretical Estimates and Corrections

5.1.1. Proper Motion

Pajdosz (1995) discusses the influence of the proper motion of the star on the measured \dot{P} :

$$\dot{P}_{\text{obs}} = \dot{P}_{\text{evol}}(1 + v_r/c) + P\dot{v}_r/c,$$

where v_r is the radial velocity of the star. Assuming $v_r/c \ll 1$, he derived

$$\dot{P}_{\text{pm}} = 2.430 \times 10^{-18} P \mu^2 d,$$

where \dot{P}_{pm} is the effect of the proper motion on the rate of period change, P is the pulsation period in seconds, μ is the proper motion in arcseconds per year, and d is the distance in parsecs. The proper motion, $\mu = 0''.136 \pm 0''.002$ yr $^{-1}$, and the parallax, $\Pi = (0''.0105 \pm 0''.0004)$, are given by van Altena et al. (1995). But the parallax has a large uncertainty and does not agree with other estimates of the distance. Munn et al. (2004) measured the same proper motion for G 117-B15A and G 117-B15B: $\mu_\alpha = (-146 \pm 2.6)$ mas yr $^{-1}$, and $\mu_\delta = (-1.0 \pm 2.6)$ mas yr $^{-1}$, including five USNO-B epochs and SDSS positions. Considering $V^A = 15.50 \pm 0.02$ (Silvestri et al. 2002), if we use the Bergeron et al. (2004) estimate of $M_V^A = 11.70 \pm 0.06^2$ derived from their optical spectra, we obtain a distance of 58 ± 2 pc, equivalent to a spectroscopic parallax of $0''.0172 \pm 0''.0005$. But G 117-B15A has *International Ultraviolet Explorer* (*IUE*) and *HST* Faint Object Spectrograph (FOS) flux-calibrated spectra (Koester et al. 1994) that can also be used to estimate the distance, if we use the evolutionary models of Wood (1995) or Panei et al. (2000) to estimate the radius from T_{eff} and $\log g$ and fit the observed fluxes to a model atmosphere calculated by Detlev Koester, similar to that described in Finley et al.

² We estimate the uncertainty in the absolute magnitude from the 300 K external uncertainty in Bergeron's temperatures.

TABLE 2
G 117-B15A DISTANCE DETERMINATIONS

Method	Distance (pc)
Parallax.....	95 ± 37
Spectroscopic parallax	58 ± 2
<i>IUE</i> flux	59 ± 5
<i>HST</i> flux	67 ± 4
Seismology from Bradley (1998).....	61
Seismology from Benvenuto et al. (2002).....	63
Mean	67 ± 14

(1997), but with an $ML2/\alpha = 0.6$ convection description consistent with Bergeron et al. (1995) and Koester & Holberg (2001). The *IUE* spectrum, recalibrated according to the New Spectroscopic Image Processing System (NEWSIPS) data reduction by NASA, was published by Holberg et al. (2003). From the *IUE* spectrum we get a distance of $d = 59 \pm 6$ pc. The *HST* spectrum, shown in Figure 3, fits a distance of $d = 67 \pm 5$ pc. Table 2 lists all the available distances to G 117-B15A.

Taking the average value of proper motion and distance, we estimate

$$\dot{P}_{\text{pm}} = (7.0 \pm 2.0) \times 10^{-16} \text{ s s}^{-1}$$

and

$$\dot{P} = \dot{P}_{\text{observed}} - \dot{P}_{\text{pm}} = (3.57 \pm 0.82) \times 10^{-15} \text{ s s}^{-1}.$$

5.2. Pulsation Models

We compare the measured value of \dot{P} with the range of theoretical values derived from realistic evolutionary models with C/O cores subject to g -mode pulsations in the temperature range of G 117-B15A. The adiabatic pulsation calculations of Bradley (1996), and Brassard et al. (1992, 1993), which allow for mode trapping, give $\dot{P} \simeq (2-7) \times 10^{-15} \text{ s s}^{-1}$ for the $\ell = 1$, low- k oscillation observed. Benvenuto et al. (2004) estimated the theoretical \dot{P} for the three modes of G 117-B15A, even allowing for a dynamical change on the gravity constant, as we show in § 1. The observed $P/\dot{P} = 1.9 \times 10^9$ yr, equivalent to 1 s change in period in 8.9 million years, is within the theoretical predictions and very close to it. We have therefore measured a rate consistent with the evolutionary timescale for this lukewarm white dwarf.

5.2.1. Core Composition

For a given mass and internal temperature distribution, theoretical models show that the rate of period change increases if the mean atomic weight of the core is increased for models that have not yet crystallized in their interiors. As the evolutionary model cools, its nucleus crystallizes due to Coulomb interactions between the ions (Lamb & van Horn 1975), and crystallization slows down the cooling by the release of latent heat. Montgomery & Winget (1999) describe the effect of crystallization on the pulsations of white dwarf stars, but G 117-B15A is not cool enough to have a crystallized core (Winget et al. 1997), or even for the convective coupling described by Fontaine et al. (2001) to occur.

The heavier the particles that compose the nucleus of the white dwarf, the faster it cools. The best estimate of mean atomic weight A of the core comes from the comparison of the observed \dot{P} with values from an evolutionary sequence of white dwarf models. Brassard et al. (1992) computed the rates of period changes for 800 evolutionary models with various masses, all with carbon

TABLE 3
DISTANCE DETERMINATIONS TO G 117-B15B

Method	Distance (pc)
Parallax.....	200 ± 280
Spectroscopic parallax.....	138 ± 47
SDSS colors.....	82
(<i>i</i> - <i>z</i>) colors.....	54
(<i>i</i> - <i>J</i>) colors.....	61
Mean.....	107 ± 62

cores but differing He/H surface layer masses, obtaining values similar to those of Winget et al. (1981), Wood & Winget (1988), and Bradley & Winget (1991). The average value of \dot{P} for all $\ell = 1, 2,$ and 3 modes with periods around 215 s in models with an effective temperature around 13,000 K, and a mass of $0.5 M_{\odot}$, is $\dot{P}(\text{C core}) = (4.3 \pm 0.5) \times 10^{-15} \text{ s s}^{-1}$. Benvenuto et al. (2004) C/O models give $\dot{P}(\text{C/O core}) = (3-4) \times 10^{-15} \text{ s s}^{-1}$. Using a Mestel-like cooling law (Mestel 1952; Kawaler et al. 1986), i.e., $\dot{T} \propto A$, where A is the mean atomic weight in the core, we can write

$$\dot{P}(A) = (3-4) \times 10^{-15} \frac{A}{14} \text{ s s}^{-1}.$$

The observed rate of period change is therefore consistent with a C or C/O core. The largest uncertainty comes from the models.

5.2.2. Reflex Motion

The presence of an orbital companion could contribute to the period change we have detected. When a star has an orbital companion, the variation of its line-of-sight position with time produces a variation in the time of arrival of the pulsation maxima, by changing the light travel time between the star and the observer by reflex motion of the white dwarf around the barycenter of the system. Kepler et al. (1991) estimated a contribution to \dot{P} caused by reflex orbital motion of the observed proper motion companion of G 117-B15A in their equation (10) as:

$$\dot{P}_{\text{orbital}} = \frac{P_{\text{pul}}}{c} \frac{GM_{\text{B}}}{a_t^2} = 1.97 \times 10^{-11} P_{\text{pul}} \frac{M_{\text{B}}/M_{\odot}}{(a_t/1 \text{ AU})^2} \text{ s s}^{-1},$$

where a_t is the total separation and M_{B} is the mass of the companion star. In the above derivation they have also assumed the orbit to be nearly edge-on to give the largest effect possible. Only the acceleration term parallel to the line of sight contributes to \dot{P} . Even though G 117-B15A and G 117-B15B are a common proper motion pair (Giclas et al. 1963),³ there is no other evidence they form a real binary system. Kotak et al. (2004) classifies G 117-B15B as an M3 Ve from its spectra, obtained with the 10 m Keck I telescope, and measured $\log g \simeq 4.5$ and $T_{\text{eff}} \simeq 3400 \text{ K}$. With $V^{\text{B}} = 16.1$ (Harrington & Dahn 1980; see footnote 3) and $M_V^{\text{B}} \simeq 10.4 \pm 0.9$ (Lang 1991) with the uncertainty coming from a possible misclassification in the spectral type of G 117-B15B from M3 V to M4 V. Such uncertainty arises from the TiO and CaOH bands seen by Kotak et al. (2004) and the $(B - V) = 1.63$ (Harrington & Dahn 1980). Its spectroscopic distance is $d^{\text{B}} = 138 \pm 47 \text{ pc}$. G 117-B15B is chromospherically

active (Kotak et al. 2004) and a flare star (Nather & Mukadam 2004). G 117-B15A and B were imaged by SDSS DR3, with $u_{\text{A}} = 15.92, g_{\text{A}} = 15.54, r_{\text{A}} = 15.64, i_{\text{A}} = 15.80, z_{\text{A}} = 16.06,$ and $u_{\text{B}} = 19.38, g_{\text{B}} = 16.95, r_{\text{B}} = 15.46, i_{\text{B}} = 13.97, z_{\text{B}} = 13.16,$ which also measure a separation of $13''.4$. They were also observed by 2MASS,⁴ with $J_{\text{A}} = 15.599 \pm 0.065, H_{\text{A}} = 15.614 \pm 0.12,$ and $J_{\text{B}} = 11.599 \pm 0.018, H_{\text{B}} = 11.156 \pm 0.12,$ and separation of $13''.4$. Using the Pickles (1998) main-sequence spectral templates convolved with SDSS filters, our best fitting template is an M4 V, with $M_V^{\text{B}} = 11.54$ and a distance of 82 pc. Using the Hawley et al. (2002) calibration for the infrared colors, G 117-B15B is consistent with the M3 V spectral type, and the (*i* - *z*) colors correspond to $M_i^{\text{B}} = 10.33,$ and a distance of 54 pc. Using the (*i* - *J*) colors, $M_i^{\text{B}} = 10.05,$ we obtain a distance of 61 pc. The parallaxes $\pi^{\text{A}} = 11 \pm 5 \text{ mas}, \pi^{\text{B}} = 5 \pm 7 \text{ mas}$ (see footnote 3), and $\pi^{\text{B}} = 4 \pm 7 \text{ mas}$ (Harrington & Dahn 1980) are too uncertain to be used to study the binary nature. Table 3 lists all the available distances to G 117-B15B.

The mass of an M3.5 V should be around $(0.30 \pm 0.03) M_{\odot}$ (Lang 1991). With a separation around $13''.4 a_t = (898 \pm 188) \text{ AU},$ corresponding to an orbital period around $(28,500 \pm 2200) \text{ yr},$ we get $\dot{P}_{\text{orbital}} \leq (1.6 \pm 1.6) \times 10^{-15} \text{ s s}^{-1}$. The large uncertainty takes into account the possibility the orbit might be strongly elliptical. Greaves (2004), in his § 4.3.1, discusses common proper motion pairs that possibly do not form a physical binary. If G 117-B15A and B form a real binary system, the contribution of an orbital reflex motion to the observed \dot{P} might account for one-half of the observed \dot{P} .

The whole observed rate of period change *could* also be caused by a planet of Jupiter's mass orbiting the white dwarf at a distance of 31 AU, which corresponds to an orbital period of 223 yr, or a smaller planet on a closer orbit (see Fig. 4). A planet with Jupiter's

⁴ See VizieR Online Data Catalog, 2246 (R. M. Cutri et al., 2003).

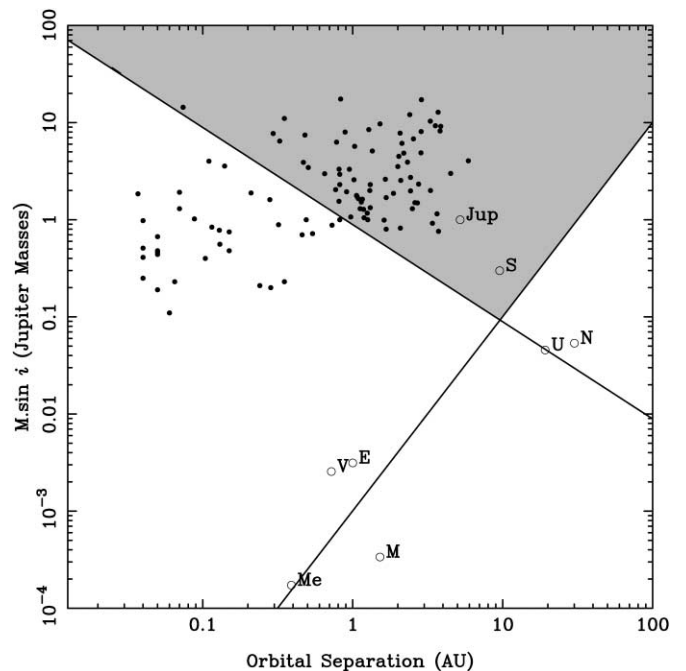


FIG. 4.—Planet exclusion region around G117-B15A. The filled dots represent known extrasolar planets around their stars, while the open circles represent solar system planets around the Sun. The short-period limit is the limit on the mass of a planet that would produce a peak in the Fourier transform smaller than those seen in Fig. 2. The long-period limit is the mass limit of a companion that would account for the observed \dot{P} . Any planet above both lines would have been detected.

³ See VizieR Online Data Catalog, 1238 (W. F. van Altena, J. T. Lee, & E. D. Hoffleit, 2001).

mass any closer to the white dwarf would lead to a larger \dot{P} . Duncan & Lissauer (1998) show that such a planet would survive the post-main-sequence mass loss. Note that reflex motion produces periodic variations on the $O - C$ times, which are distinguishable from parabolic variations after a significant portion of the orbit has been covered.

As discussed by Damour & Taylor (1991), any relative acceleration of the star with respect to the barycenter of the solar system will contribute to the observed \dot{P} . Their equations (2.2) for the differential galactic orbits, decomposed in a planar contribution (2.12), where the second term is the proper motion correction, and a perpendicular contribution (2.28), applied to G 117-B15A, show the galactic contribution to be exactly the one calculated above for proper motion, i.e., the other terms are negligible (2 to 3 orders of magnitude smaller).

6. CONCLUSIONS

We have measured the rate of change of the main pulsation period for the $T_{\text{eff}} \simeq 12,000$ K pulsating DA white dwarf G 117-B15A, the first ZZ Ceti to have its evolutionary rate of change measured, confirming it is the most stable optical clock known, with a rate of change of 1 s in 8.9 million years and a precise laboratory for physics at high energy. It is important to notice that mode trapping, a resonance between the local pulsation wavelength with the thickness of one of the compositional layers, can reduce the rate of period change by up to a factor of 2 (Bradley 1996), but the changes in the trapping layers are still caused by cooling.

It has taken a huge investment of telescope time to achieve such precision, but not only have we measured the cooling rate of this 400 million year old white dwarf (Wood 1995), excluding the time the star took to reach the white dwarf phase, we have also demonstrated that it does not harbor Jupiter-mass planetary bodies up to a distance around 30 AU from the star, or smaller planets with light travel time effects larger than 1 s.

We claim that the 215 s periodicity in G 117-B15A is the most stable optical clock known. Santra et al. (2005) and Hoyt et al. (2005) discuss projects to build optical atomic clocks based on single trapped ions, or several laser-cooled neutral atoms, of strontium or ytterbium, expected to reach an accuracy of $\dot{P} \leq 2 \times 10^{-17} \text{ s s}^{-1}$. Considering their periods are 2.5×10^{-15} and 1.9×10^{-13} s, even though they will be more accurate than G 117-B15A, they will be much less stable, as their timescales for period changes, P/\dot{P} , are 125 s and 3 hr, compared to 2 Gyr for G 117-B15A. Even the Hulse & Taylor millisecond pulsar (Hulse & Taylor 1975) has a timescale for period change of only 0.35 Gyr (Damour & Taylor 1991), but the radio millisecond pulsar PSR J1713+0747 (Splaver et al. 2005) has $\dot{P} = 8.1 \times 10^{-21} \text{ s s}^{-1}$, and a timescale of 8 Gyr, and PSR B1885+09 = PSR J1857+0943 with $\dot{P} = 1.78363 \times 10^{-20} \text{ s s}^{-1}$ has a stability timescale of 9.5 Gyr (Kaspi et al. 1994). Together with these millisecond pulsars, G 117-B15A may be used as the most stable known natural frequency and time-keeping standards (e.g., Kopeikin & Potapov 2004). The white dwarf has the advantage of not having glitches and less severe general relativistic corrections.

It is essential to note that the measured rate of period change is consistent with the cooling rate in our white dwarf models only for cores of C or C/O. With the refinement of the models, the observed rate of period change can be used to accurately measure the ratio of carbon to oxygen in the core of this normal white dwarf, and therefore help in constraining the $C(\alpha, \gamma)O$ cross section.

This work was partially supported by grants from CNPq (Brazil), FINEP (Brazil), NSF (USA), and NASA (USA). This research has made extensive use of NASA's Astrophysical Data System Abstract Service.

REFERENCES

- Benvenuto, O. G., Córscico, A. H., Althaus, L. G., & Serenelli, A. M. 2002, *MNRAS*, 332, 399
- Benvenuto, O. G., García-Berro, E., & Isern, J. 2004, *Phys. Rev. D*, 69, 082002
- Bergeron, P., Fontaine, G., Billères, M., Boudreault, S., & Green, E. M. 2004, *ApJ*, 600, 404
- Bergeron, P., Wesemael, F., Lamontagne, R., Fontaine, G., Saffer, R. A., & Allard, N. F. 1995, *ApJ*, 449, 258
- Biesiada, M., & Malec, B. 2002, *Physical Review D*, 65, 43008
- Bradley, P. A. 1996, *ApJ*, 468, 350
- . 1998, *ApJS*, 116, 307
- Bradley, P. A., & Winget, D. E. 1991, *ApJS*, 75, 463
- Brassard, P., Fontaine, G., Wesemael, F., & Talon, A. 1993, in *White Dwarfs: Advances in Observation and Theory*, ed. M. A. Barstow (Dordrecht: Kluwer), 485
- Brassard, P., Fontaine, G., Wesemael, F., & Tassoul, M. 1992, *ApJS*, 81, 747
- Córscico, A. H., Benvenuto, O. G., Althaus, L. G., Isern, J., & García-Berro, E. 2001, *NewA*, 6, 197
- Costa, J. E. S., Kepler, S. O., & Winget, D. E. 1999, *ApJ*, 522, 973
- Damour, T., & Taylor, J. H. 1991, *ApJ*, 366, 501
- Duncan, M. J., & Lissauer, J. J. 1998, *Icarus*, 134, 303
- Eggen, O. J., & Greenstein, J. L. 1965, *ApJ*, 141, 83
- Finley, D. S., Koester, D., & Basri, G. 1997, *ApJ*, 488, 375
- Fontaine, G., Brassard, P., & Bergeron, P. 2001, *PASP*, 113, 409
- Giclas, H. L., Burnham, R., & Thomas, N. G. 1963, *Lowell Observatory Bulletin*, 6, 1
- Greaves, J. 2004, *MNRAS*, 355, 585
- Harrington, R. S., & Dahn, C. C. 1980, *AJ*, 85, 454
- Hawley, S. L., et al. 2002, *AJ*, 123, 3409
- Holberg, J. B., Barstow, M. A., & Burleigh, M. R. 2003, *ApJS*, 147, 145
- Hoyt, C. W., Barber, Z. W., Oates, C. W., Fortier, T. M., Diddams, S. A., & Hollberg, L. 2005, *Phys. Rev. Lett.*, 95, 083003
- Hulse, R. A., & Taylor, J. H. 1975, *ApJ*, 195, L51
- Isern, J., García-Berro, E., Corsico, A. H., Benvenuto, O. G., & Althaus, L. G. 2004, *Commun. Asteroseismology*, 145, 13
- Kaspi, V. M., Taylor, J. H., & Ryba, M. F. 1994, *ApJ*, 428, 713
- Kawaler, S. D., Winget, D. E., Iben, I., & Hansen, C. J. 1986, *ApJ*, 302, 530
- Kepler, S. O. 1984, *ApJ*, 286, 314
- . 1993, *Baltic Astron.*, 2, 515
- . 2004, *International J. Mod. Phys. D*, 13, 1493
- Kepler, S. O., Mukadam, A., Winget, D. E., Nather, R. E., Metcalfe, T. S., Reed, M. D., Kawaler, S. D., & Bradley, P. A. 2000, *ApJ*, 534, L185
- Kepler, S. O., Robinson, E. L., & Nather, R. E. 1983, *ApJ*, 271, 744
- Kepler, S. O., Robinson, E. L., Nather, R. E., & McGraw, J. T. 1982, *ApJ*, 254, 676
- Kepler, S. O., et al. 1991, *ApJ*, 378, L45
- . 1995, *Baltic Astron.*, 4, 221
- Kleinman, S. J., et al. 2004, *ApJ*, 607, 426
- Koester, D., Allard, N. F., & Vauclair, G. 1994, *A&A*, 291, L9
- Koester, D., & Holberg, J. B. 2001, in *ASP Conf. Ser. 226, 12th European Workshop on White Dwarfs*, ed. J. L. Provencal, H. L. Shipman, J. MacDonald, & S. Goodchild (San Francisco: ASP), 299
- Kopeikin, S. M., & Potapov, V. A. 2004, *MNRAS*, 355, 395
- Kotak, R., van Kerkwijk, M. H., & Clemens, J. C. 2004, *A&A*, 413, 301
- Lamb, D. Q., & van Horn, H. M. 1975, *ApJ*, 200, 306
- Lang, K. R. 1991, *Astrophysical Data: Planets and Stars* (New York: Springer), 145
- Mestel, L. 1952, *MNRAS*, 112, 583
- McGraw, J. T. 1979, *ApJ*, 229, 203
- McGraw, J. T., & Robinson, E. L. 1976, *ApJ*, 205, L155
- Montgomery, M. H., & Winget, D. E. 1999, *ApJ*, 526, 976
- Mukadam, A. S., Winget, D. E., von Hippel, T., Montgomery, M. H., Kepler, S. O., & Costa, A. F. M. 2004a, *ApJ*, 612, 1052
- Mukadam, A. S., et al. 2003, *ApJ*, 594, 961
- . 2004b, *ApJ*, 607, 982
- Mullally, F., Thompson, S. E., Castanheira, B. G., Winget, D. E., Kepler, S. O., Eisenstein, D. J., Kleinman, S. J., & Nitta, A. 2005, *ApJ*, 625, 966

- Munn, J. A., et al. 2004, *AJ*, 127, 3034
- Nather, R. E., & Mukadam, A. S. 2004, *ApJ*, 605, 846
- Nather, R. E., Winget, D. E., Clemens, J. C., Hansen, C. J., & Hine, B. P. 1990, *ApJ*, 361, 309
- O'Donoghue, D. 1994, *MNRAS*, 270, 222
- Pajdosz, G. 1995, *A&A*, 295, L17
- Panei, J. A., Althaus, L. G., & Benvenuto, O. G. 2000, *A&A*, 353, 970
- Pickles, A. J. 1998, *PASP*, 110, 863
- Robinson, E. L. 1979, in *Proc. IAU Colloq. 53, White Dwarfs and Variable Degenerate Stars*, ed. H. M. Van Horn & V. Weidemann (Rochester: Univ. Rochester), 343
- Robinson, E. L., Kepler, S. O., & Nather, R. E. 1982, *ApJ*, 259, 219
- Robinson, E. L., et al. 1995, *ApJ*, 438, 908
- Santra, R., Arimondo, E., Ido, T., Greene, C. H., & Ye, J. 2005, *Phys. Rev. Lett.*, 94, 173002
- Silvestri, N. M., Oswalt, T. D., & Hawley, S. L. 2002, *AJ*, 124, 1118
- Splaver, E. M., Nice, D. J., Stairs, I. H., Lommen, A. N., & Backer, D. C. 2005, *ApJ*, 620, 405
- Standish, E. M. 1998, *A&A*, 336, 381
- . 2004, *A&A*, 417, 1165
- van Altena, W. F., Lee, J. T., & Hoffleit, E. D. 1995 (4th ed.; New Haven: Yale Univ. Observatory), stars 2232.01
- Winget, D. E., Hansen, C. J., & van Horn, H. M. 1983, *Nature*, 303, 781
- Winget, D. E., Kepler, S. O., Kanaan, A., Montgomery, M. H., & Giovannini, O. 1997, *ApJ*, 487, L191
- Winget, D. E., van Horn, H. M., & Hansen, C. J. 1981, *ApJ*, 245, L33
- Wood, M. A. 1995, in *Proc. 9th European Workshop on White Dwarfs*, ed. D. Koester & K. Werner (Berlin: Springer), 41
- Wood, M. A., & Winget, D. E. 1988, in *Multimode Stellar Pulsations*, ed. G. Kovacs, L. Szabados, & B. Szeidl (Budapest: Konkoly Obs.), 199